# A role of the Nse4 kleisin and Nse1/Nse3 KITE subunits in the ATPase cycle of SMC5/6

Vondrova L. [1], Adamus M. [2], Nociar M. [1], Kolesar P. [1], Oliver A.W. [3], Palecek J.J. [1,2]

[1] National Centre for Biomolecular Research, Faculty of Science, Masaryk University, Kotlarska 2, 61137 Brno, Czech Republic

[2] Mendel Centre for Plant Genomics and Proteomics, Central European Institute of Technology, Masaryk University, Kamenice 5, 62500 Brno, Czech Republic

[3] Genome Damage and Stability Centre, School of Life Sciences, University of Sussex, Falmer, Brighton BN1 9RQ, United Kingdom

Corresponding address: jpalecek@sci.muni.cz; Tel.: +420-54949-6128

Keywords: SMC5/6 complex; Nse4 klesin linker; Nse1/Nse3 KITE subunits; ATP binding; protein-protein interaction, fission yeast

## ABSTRACT

The SMC (Structural Maintenance of Chromosomes) complexes are composed of SMC dimers, kleisin and kleisin-interacting subunits. Mutual interactions of these subunits constitute the basal architecture of the SMC complexes. Particularly, terminal domains of the kleisin subunit bridge the SMC head domains of the SMC molecules. Binding of ATP molecules to the heads and their hydrolysis alter the shape of long SMC molecules (from rod-like to open-ring shapes) and power them with motor activity. The kleisin-interacting (HAWK or KITE) subunits bind kleisin linker regions and regulate such dynamic activities.

We developed new systems to follow the interactions between SMC5/6 subunits and stability of the SMC5/6 complexes. First, we show that the N-terminal domain of the Nse4 kleisin molecule binds to the SMC6 neck and bridges it to the SMC5 head. Second, binding of the Nse1 and Nse3 KITE proteins to the Nse4 linker part increases stability of the ATP-free SMC5/6 complex. In contrast, binding of ATP to the SMC5/6 complex containing KITE subunits significantly decreases its stability. Elongation of the Nse4 linker partially suppresses instability of the ATP-bound complex, suggesting that the binding of the KITE proteins to the Nse4 linker constrains its limited size. Our data suggest that the KITE proteins may shape the Nse4 linker to fit the ATP-free complex optimally and to facilitate opening of the complex upon ATP binding. This mechanism suggests an important role of the KITE subunits in the dynamics of the SMC5/6 complexes.

## AUTHOR SUMMARY

The SMC5/6 complex is member of the Structural maintenance of chromosomes (SMC) family, key organizers of both prokaryotic and eukaryotic genomes. Their architecture and dynamics (driven by ATP binding and hydrolysis) are essential for cellular processes, like

chromatin segregation, condensation, replication and repair. In this paper, we described conserved mode of the Nse4 kleisin subunit binding to the SMC6 (similar to cohesin and condensin) and its bridging role. Furthermore, we showed different impact of the binding of the Nse1-Nse3 KITE subunits to the Nse4 kleisin bridge. Our study suggested that the KITE proteins modulate the stability of the SMC5/6 complex, depending on its binding and hydrolysis of ATP. Our findings uncover molecular mechanisms underlying dynamics of the SMC5/6 complexes.

## INTRODUCTION

The SMC (Structural Maintenance of Chromosomes) complexes are key organizers of prokaryotic and eukaryotic genomes. They organize chromatin domains (cohesins; [1]), condense mitotic chromosomes (condensins; [2]), assist in DNA repair (SMC5/6; [3, 4]) and replication (SMC/ScpAB; [5]). These circular complexes use the energy of ATP hydrolysis to drive DNA topology changes. In prokaryotes, SMC/ScpAB drives extrusion of loops forming behind the replication fork. In eukaryotes, condensins extrude loops laterally and axially to shape chromatin to the typical mitotic chromosomes. Cohesins assist in formation of topologically associating domains during interphase. Cohesin rings can also hold newly replicated sister chromatids together and release them in highly controlled manner. The SMC5/6 complexes have been implicated in the repair of DNA damage by homologous recombination, stabilization and restart of stressed replication forks. The SMC5/6 instability leads to the chromosome breakage syndrome in human [6], however, the molecular mechanism of the SMC5/6 action is largely unclear.

All the SMC complexes are composed of three common categories of subunits: SMC, kleisin and kleisin-interacting proteins [7, 8]. The SMC proteins are primarily build of long anti-parallel coiled-coil arms, a globular hinge (situated in the middle of their peptide chain)

64 and a head domain (formed by combined amino and carboxyl termini; [9-13]). The globular
65 head domain contains ATP binding and hydrolysis motifs of the ATP-binding cassette
66 transporter family [14, 15]. Two SMC molecules form dimers via the association of their hinge
67 domains and transiently interact when their head domains sandwich a pair of ATP molecules.
68 The binding of ATP changes conformation and shape of the SMC subunits at local as well as
69 global levels [10]. At local level, the SMC heads and necks move from aligned position to the
70 ATP-locked conformation. At global level, the overall shape of the complex changes from rod-
71 to ring-like upon ATP binding (with heads locked by ATP at one end and hinge dimer at the
72 other end). The hydrolysis of ATP dissolves the SMC-ATP-SMC head bridge.

73 The ATPase head domains are also connected by the kleisin subunit in an asymmetric
74 way. Kleisin binds to the cap side of one SMC (designated as κSMC) head domain via a
75 winged-helix domain (WHD) at its carboxyl terminus. Kleisin's α-helix located at its amino
76 terminal helix-turn-helix (HTH) domain binds to the coiled-coil base region immediately
77 adjacent to the other SMC head (called neck and designated as νSMC; [16-18]). This kleisin
78 bridge mediated by protein-protein interactions seems to be more permanent than the ATP-
79 mediated bridge (as the latter bridge dissolves upon ATP hydrolysis). However, the ATP
80 binding may induce dissociation of the kleisin-νSMC interaction and lead to release of DNA
81 from cohesin ring [19-24].

82 The kleisin-interacting subunits bind and shape kleisin linker regions conecting N-
83 (HTH) and C-terminal (WHD) domains. The KITE (Kleisin-Interacting Tandem winged-helix
84 Element) subunits interact with kleisins in prokaryotic SMC/ScpAB and eukaryotic SMC5/6
85 complexes, while eukaryotic cohesin and condensin complexes associate with HAWK (HEAT
86 proteins Associated With Kleisin) proteins. Interestingly, HAWK (Scc3 and Pds5) and Wapl
87 proteins regulate release of cohesin from chromosomes. It was proposed that these proteins
88 shape and stiffen the linker region of kleisin molecule, which assists in transduction of

89 conformational changes of the ATP-mediated SMC head dimerization to the dissociation of the
90 kleisin-νSMC interaction (Scc1-Smc3 in the cohesin complex). Similarly, KITE proteins assist
91 in opening of the SMC/ScpAB complex [25, 26]. However, the role of the KITE subunits in the
92 SMC5/6 complex remains largely elusive.

93 Here we aimed to uncover relationships between SMC5/6 subunits and their roles in the
94 SMC5/6 dynamics. We developed new systems to analyse the interactions between SMC5/6
95 subunits and to follow the stability of SMC5/6 complexes. Using systems composed of SMC6-
96 Nse4-Nse3-Nse1 and SMC6-Nse4-SMC5, respectively, we showed that the N-terminal HTH
97 domain of the Nse4 kleisin molecule binds to the SMC6 neck and bridges it with the SMC5
98 head. With a more complex system, we observed increased stability of the ATP-free SMC5/6
99 complex upon binding of the Nse1 and Nse3 KITE proteins to the Nse4 kleisin. While the ATP-
100 free complex was highly stable, the binding of ATP to the SMC5/6 complex containing KITE-
101 bound kleisin significantly decreased its stability. Reduced Nse3 binding to the Nse4 linker or
102 elongation of the Nse4 linker partially suppressed the instability of the ATP-bound complex,
103 suggesting that the binding of the KITE proteins to the Nse4 linker constrains its limited size.
104 Our data suggest that the KITE proteins may shape the Nse4 linker to fit the ATP-free complex
105 optimally and to facilitate opening of the complex upon ATP binding.

106

107 **RESULTS**

108 **Nse4 interacts with SMC6 neck**

109 We have previously shown that Nse4 belongs to the kleisin superfamily of proteins and
110 binds to SMC5 and SMC6 head fragments [27]. To map Nse4 interactions with SMC6, we
111 employed peptide libraries covering yeast *S. pombe* SMC6 regions aa 241-365 and aa875-1024
112 (Suppl. Fig. S1A and Supplementary Table 1; unpublished data). The peptides were pre-bound

113 to ELISA plates and tested against Nse4(1-150) and control (human TRF2) protein [28, 29].
114 The peptides covering the C-terminal region of SMC6 (aa955-1009) bound to Nse4 (Figs. 1A
115 and S1A). The peptide aa960-984 exhibited the highest affinity and specificity to Nse4 while
116 other peptides bound to Nse4 in a less specific way (e.g. peptide aa970-994). Interestingly, the
117 SMC6 region aa960-984 corresponds to the SMC neck regions interacting with kleisins in most
118 SMC complexes [12].

119 To analyse the Nse4-SMC6 interaction in more detail, we established various
120 multicomponent yeast two-hybrid (mY2H) systems [30]. It was difficult to follow the Nse4-
121 SMC6 binary interaction in classical Y2H (Fig. 1B, column 3; [27, 31, 32]), therefore we added
122 DNA encoding Nse1 and Nse3 subunits on an extra plasmid (p416ADH1-Nse1+Nse3
123 construct, 4Y2H) to enhance Nse4-binding properties [33]. Indeed, addition of both Nse1 and
124 Nse3 subunits to Gal4BD-Nse4/Gal4AD-SMC6 resulted in a stable SMC6-Nse4-Nse3-Nse1
125 complex (Fig. 1B, column 4). Similarly, addition of SMC5 to Nse4-SMC6 (3Y2H) resulted in
126 formation of a stable SMC5-Nse4-SMC6 complex (Fig. 1C, column 4).

127 Using these mY2H systems and site-directed mutagenesis, we aimed to identify the
128 Nse4-binding residues within the most conserved part of the ELISA-defined SMC6 region
129 (aa960-984; Figs. 1A and S1B; unpublished data). The L964A, L965A, L968A, E969A, L972A
130 and R975A mutations reduced stability of the SMC6-Nse4-Nse3-Nse1 tetramer while the others
131 had negligible effect (Figs. 1B and S1C). These data suggest that residues L964, L965, L968,
132 E969, L972 and R975 may mediate either the Nse4-SMC6 interaction or putative interactions
133 between SMC6 and Nse1-Nse3 subunits. To exclude the latter possibility, we employed 3Y2H
134 system consisting of the SMC5/SMC6/Nse4 subunits. Again, L964A, L965A, L968A, E969A,
135 L972A and R975A mutations reduced stability of the (SMC5-)SMC6-Nse4 complex while the
136 others had no effect (Figs. 1C and S1D), suggesting that these residues may mediate Nse4-
137 SMC6 interaction.

138 To distinguish between mutations specifically disturbing the Nse4-SMC6 interaction
139 from those affecting SMC6 structure, we established another 3Y2H system consisting of SMC6
140 and Nse5-Nse6 subunits (as Nse5 and Nse6 bind to the SMC6 protein; [27]). In this system, we
141 used the same Gal4AD-SMC6 mutation constructs as above in combination with Gal4BD-Nse5
142 and p416ADH1-Nse6 (Figs. 1D and S1E). The mutations L964A, L968A and E969A reduced
143 SMC6-Nse5-Nse6 complex stability, suggesting their deleterious effect on SMC6 structure
144 (Fig. 1, compare panels B, C and D, columns 5, 7 and 8). In contrast, the other mutations had
145 no impact, suggesting that the conserved L965, L972 and R975 residues within the SMC6 neck
146 region mediate SMC6-Nse4 interaction (Figs. 1 and S1).

147

148 **SMC6 binds N-terminal motif of Nse4 protein**

149 Next, we took advantage of the crystal structures of the kleisin-νSMC complexes [16-
150 18, 26, 34], which suggest a key role for the N-terminal HTH domain of the kleisin molecule
151 in its binding to νSMC neck. We mutated residues within the third α-helix of the Nse4 HTH
152 domain (aa62-68) and analysed their impact on the Nse4-SMC6 interaction using the SMC5-
153 Nse4-SMC6 3Y2H system as above (Fig. 1C). The Nse4 mutations L62C, K64C, T65R, D67C
154 and L68C reduced the SMC5-Nse4-SMC6 stability significantly while the others had no effect
155 (Fig. 2A). To distinguish between mutations specifically disturbing Nse4-SMC6 interactions
156 and mutations affecting Nse4 structure, we tested the Gal4BD-Nse4 mutation constructs in
157 combination with Gal4AD-Nse3 in the classical Y2H system (Fig. 2B; [28, 35]). The K64C
158 and D67C mutations affected the Nse3-Nse4 interaction, suggesting their deleterious effect on
159 the Nse4 structure (Fig. 2B, columns 6 and 9). In contrast, the other mutations had no effect on
160 the Nse3-Nse4 interaction, suggesting that the intact L62, T65 and L68 conserved residues are
161 required for the Nse4-SMC6 binding (Fig. 2C). Altogether, our data suggest that the Nse4 HTH

162 motif binds the SMC6 neck region and that the SMC6-Nse4 interaction mode is similar to the
163 other νSMC-kleisin interactions [12, 13].

164 To analyse the role of the Nse4-SMC6 interaction in yeast cells, we introduced the L62C
165 and T65R mutations into the genome of diploid *S. pombe*. Tetrad analysis showed that the single
166 *nse4-T65R* and double *nse4-L62C, T65R* mutations were lethal (Fig. 2D), suggesting an
167 essential role for the Nse4-SMC6 interaction.

168

169 **A role for the Nse4 and ATP molecules in bridging of SMC5-SMC6**

170 To compare the role of Nse4 and ATP in bridging of the SMC5-SMC6 heads, we
171 introduced the SMC5/E995Q mutation which inhibits ATP hydrolysis; i.e. enhances ATP
172 retention between SMC5-SMC6 heads and their dimerization (Figs. 3A and S2; [14, 36]). In
173 the 3Y2H system, the interaction between Gal4BD-SMC5 and Gal4AD-SMC6 constructs was
174 not detectable, suggesting a low stability of the SMC5-SMC6 dimer even upon stable binding
175 of ATP (Fig. 3A, columns 1 and 2). Addition of Nse4 resulted in stable SMC5-Nse4-SMC6
176 complex formation (Fig. 3A, columns 3 and 4), suggesting that Nse4 stabilizes the bridge
177 between SMC5 and SMC6. The introduction of the ATP-hydrolysis mutation to the SMC5-
178 Nse4-SMC6 complex only slightly increased its stability (Fig. 3A), suggesting a major role of
179 Nse4 (and a minor additive effect of ATP binding; see below) in bridging of the SMC5-SMC6
180 heads.

181 When we reduced the Nse4 binding affinity to SMC6 using the specific Nse4 mutations
182 described above, the stability of the wild-type SMC5 complexes dropped more dramatically
183 than the stability of the SMC5/E995Q mutant complexes (Fig. 3A, compare odd and even
184 columns). For example, the L68C mutation reduced stability of the wild-type SMC5-Nse4-
185 SMC6 complex significantly while the ATP molecule (in SMC5/E995Q) stabilized the
186 Nse4/L68C complex (Fig. 3A, columns 5 and 6). Further reduction of the Nse4 binding affinity

187 (Fig. 3A, columns 7-12) led to further drops in stability of SMC5-Nse4-SMC6, again, with
188 more stable hydrolytic mutants. Although the stability of the Nse4/L62C, T65R double mutant
189 complex was very low, the residual affinity of Nse4 to SMC6 still supported ATP binding in
190 the SMC5/E995Q mutant (Fig. 3A, columns 11 and 12). These data suggest that ATP
191 contributes significantly to the SMC5-SMC6 bridging when the Nse4 affinity is reduced and
192 that the Nse4 and ATP interactions are synergistic in the SMC5-Nse4-SMC6 complex.

193

194 **KITE-bound Nse4 is constrained upon ATP binding**

195 To analyse the role of ATP binding to SMC5-SMC6 within the complex stabilized by
196 KITE proteins, we added Nse1 and Nse3 to the p416ADH1-Nse4 plasmid (p416ADH1-
197 Nse4+Nse3+Nse1 construct, 5Y2H; Fig. 3B; [30, 37]). Consistent with their Nse4-stabilizing
198 roles (Fig. 1B), the KITE proteins increased the stability of the SMC5-Nse4-SMC6 complex
199 significantly (Fig. 3B, compare columns 1 and 3). Surprisingly, addition of the SMC5/E995Q
200 ATP-hydrolysis mutation greatly destabilized the SMC5-SMC6-Nse4-Nse3-Nse1 complex
201 (Fig. 3B, compare columns 3 and 4), suggesting antagonistic roles of ATP and KITE subunits.

202 To ensure that the instability of the ATP-bound SMC5-SMC6-Nse4-Nse3-Nse1
203 complex is specifically caused by the ATP-mediated SMC5-SMC6 head bridge, we introduced
204 either SMC6/S1045R mutation disturbing the ATP-mediated SMC5-SMC6 dimerization
205 interface or SMC5/K57I mutation abolishing binding of ATP (Suppl. Fig. S2; [14, 36, 38]). As
206 the SMC6/S1045R mutation suppressed instability caused by the SMC5/E995Q mutation
207 (Suppl. Fig. S2, column 10), we can exclude a direct impact of this mutation on SMC5 (e.g. on
208 SMC5-Nse4 interaction). The observation that both mutations suppressed instability caused by
209 the SMC5/E995Q mutation (Suppl. Fig. S2, column 10 and 12) confirm the notion that ATP-
210 mediated SMC5-SMC6 head dimerization causes SMC5-SMC6-Nse4-Nse3-Nse1 instability.

211 Given that both ATP and Nse4 bridge SMC5-SMC6 heads, our data suggest that ATP
212 constrains KITE-bound Nse4 bridge (and vice versa; Fig. 3B, compare columns 2 and 4).
213 Therefore, we reduced Nse4 binding affinity to SMC6 (to release the constraint) using the
214 specific Nse4 mutations described above (Figs. 2 and 3A). With decreasing Nse4 affinity, the
215 stability of the ATP-free complexes gradually dropped to its limit (Fig. 3B, columns 5, 7, 9 and
216 11), suggesting that only Nse4 brought SMC5-SMC6 together. In contrast, the stability of the
217 ATP-bound SMC5-SMC6-Nse4-Nse3-Nse1 complexes dropped first (columns 6, 8, and 10)
218 and then it partially recovered in the L62C, T65R double mutant (column 12). In the single
219 mutants, the reduced Nse4 binding affinity (balance between the Nse4 binding and competing
220 binding of ATP) resulted in decreased stability of these complexes. In the double mutant,
221 residual Nse4 binding was too weak to compete the ATP binding and therefore ATP became
222 the major bridge (manifested as increased stability of the SMC5-SMC6-Nse4-Nse3-Nse1
223 complex). These data suggest that ATP constrains KITE-bound Nse4 bridge (and vice versa;
224 i.e. the stability of the KITE-containing SMC5/6 complexes depends on the balance between
225 the Nse4 binding and competing binding of ATP).

226

227 **The ATP-mediated constraint depends on the KITE subunits**

228 In the SMC5/6 complex, KITE and kleisin subunits form a tight Nse1-Nse3-Nse4 sub-
229 complex mediated by their mutual interactions (Fig. 4A; [27, 35]). As ATP destabilized the
230 Nse4 bridge only in the presence of the KITE subunits (Fig. 3), we introduced mutations
231 specifically affecting stability of the Nse1-Nse3-Nse4 trimer to evaluate a role of the KITE
232 proteins. Specific mutations disturbing only individual Nse1-Nse3 (Nse1/Q18A, M21A) and
233 Nse3-Nse4 (Nse4/del87-91) binary interactions (Fig. 4A, compare columns 3 against 4 and 9
234 against 10) did not affect the stability of the whole Nse1-Nse3-Nse4 trimer (Fig. 4A, columns
235 6 and 7), but their combination compromised trimer assembly (Fig. 4A, column 8). When we

236 introduced this combination of Nse1 and Nse4 mutations to the SMC5-SMC6-Nse4-Nse3-Nse1
237 complex, its stability was reduced as the KITE proteins lost their ability to bind and stabilize
238 Nse4 (Fig. 4B, compare columns 6 and 8). In contrast, when we introduced this combination of
239 Nse1 and Nse4 mutations to the SMC5/E995Q hydrolytic mutant complex, the stability of the
240 ATP-bound complex was increased (Fig. 4B, compare columns 7 and 9), suggesting that the
241 ATP-induced constraint of Nse4 depends on its binding to the KITE subunits. Importantly, there
242 was no difference between the stability of the ATP-free and ATP-bound complexes (compare
243 columns 8 and 9), further corroborating our conclusion that the ATP-mediated constraint
244 depends on the binding of KITE dimer to Nse4. Furthermore, the Nse4/del87-91 mutation
245 compromising only Nse3-Nse4 interaction (Figs. 4A, columns 4 and 6) had a suppressing effect
246 on SMC5/E995Q complex similar to the double mutant (Fig. 4B, compare columns 9 and 11),
247 suggesting that the binding of Nse3 to the Nse4 linker partially constrained it. Our data suggest
248 that the instability of the SMC5/6 complex induced by ATP binding is dependent on the binding
249 of KITE proteins to the Nse4 kleisin linker.

250

251 **The limited size of the Nse4 linker poses mechanical constraint**

252 The KITE dimers bind linker regions of kleisin molecules in SMC complexes [7, 16,
253 28, 39-41]. To explore the role of the Nse4 linker in propagation of the ATP-induced constraint,
254 we inserted a 30 amino acid extension at the putative end of the linker (Fig. 4C; [27]) to lengthen
255 the linker. The Nse4 extended construct bound Nse1-Nse3 KITE proteins normally (Fig. 4D)
256 and formed the SMC5-SMC6-Nse4-Nse3-Nse1 complex with the stability similar to that with
257 the normal Nse4 construct (Fig. 4E, columns 3 and 4). Interestingly, combination of the Nse4
258 extended construct with the SMC5/E995Q ATP-hydrolysis mutant increased the stability of the
259 SMC5-SMC6-Nse4-Nse3-Nse1 complex, suggesting that the extended Nse4 linker partially
260 alleviated ATP-induced constraint (Fig. 4E, columns 5 and 6).

261 Taken together, we propose a model in which the KITE proteins shape the kleisin linker
262 connecting SMC heads. The KITE-shaped Nse4 linker fits the ATP-free conformation of
263 SMC5/6 (and therefore increases its stability), while the ATP-bound conformation is not
264 compatible with the KITE-shaped Nse4 linker (and therefore constrains the Nse4 bridge; Fig.
265 5). This model suggests a key role of the kleisin and KITE subunits in molecular mechanisms
266 driving the SMC5/6 dynamics.

267

268 **DISCUSSION**

269 The kleisin subunits bridge the SMC heads in an asymmetric way and lock the SMC
270 ring at its head side [12, 13]. We have shown that Nse4 belongs to the kleisin superfamily of
271 proteins and binds strongly to κSMC5 head via its Nse4 C-terminal WHD [27]. However, we
272 observed only weak binding of Nse4 to νSMC6 [27] and other studies actually failed to show
273 the Nse4-SMC6 interaction [31, 32, 42]. Here we developed several systems to prove and
274 analyse the interaction between Nse4 and SMC6. We mapped the Nse4-SMC6 interface in
275 detail and found that the Nse4-SMC6 interaction mode is similar to the other νSMC-kleisin
276 interactions [16-18, 26, 34]. Therefore, we assume that Nse4 bridges SMC5-SMC6 proteins in
277 a way similar to kleisins in the other SMC complexes, except that the Nse4 bridge is specifically
278 modulated by the Nse1-Nse3 KITE subunits in the SMC5/6 complex (see below).

279 The kleisins lock the SMC rings that can embrace DNA or extrude a loop in an ATP-
280 dependent way [43]. To release such entrapped DNA (or extrude the loop), the SMC-SMC or
281 SMC-kleisin interface must be open. It was proposed that the νSMC-kleisin interface opens
282 and serves as an exit gate for trapped DNA [19, 44, 45]. In the cohesin complex, the Scc1-
283 SMC3 interface is opened upon ATP binding (in the presence of the Pds5 and Wapl regulators;
284 [19-24]). Our data show that the SMC5/6 complex is unstable in the ATP-bound state,

285 suggesting that one or more interfaces are compromised upon ATP binding (Fig. 3B). Given
286 the weak nature of the Nse4-SMC6 interaction, we assume that this interaction is prone to
287 dissociation and that the Nse4-SMC6 interface is opened upon ATP binding. Consistent with
288 the latter notion, the ATP-mediated constraint was released when the Nse4-SMC6 interaction
289 was disturbed (Fig. 3B). Therefore, we hypothesize that the binding of ATP to the SMC5-SMC6
290 heads constrains the Nse4 bridge (when bound by the Nse1 and Nse3 KITE subunits; see below
291 and Fig. 5) and this constraint is released via dissociation of the Nse4-SMC6 interaction (Fig.
292 3B).

293 The ATP binding induces changes in the mutual positions (and conformations) of the
294 SMC heads and arms [10, 26, 46-48]. Consequently, the shape of the whole SMC complex
295 changes from a rod-like conformation (with juxtaposed arms stabilized by their mutual
296 interactions) to the less stable open ring (Fig. 5). At least part of the ATP-induced SMC5/6
297 instability (Fig. 3B) might be a consequence of the shape transition from rod to ring (our
298 electron microscopy data suggest that the human SMC5/6 complex can adopt both shapes; M.
299 Adamus, unpublished data). However, we observed this instability only in the presence of the
300 KITE subunits, suggesting that either our system is unable to detect the SMC5-SMC6 rod-to-
301 ring shape transition (and monitors only Nse4 bridge opening) or the KITE proteins are required
302 for the full rod-to-ring shape transition. The latter possibility is consistent with the prokaryotic
303 SMC/ScpAB data which suggest an important function of the KITE subunits in pulling SMC
304 arms [25, 26]. In our model, the binding of ATP to the SMC5-SMC6 heads pulls their arms
305 apart and constrains the KITE-bound Nse4 bridge (Fig. 5).

306 It was shown that kleisin-interacting proteins (particularly KITE and HAWK subunits)
307 bind and shape linker regions of the kleisin molecules [7, 11, 16, 28, 39-41, 49-51]. Our data
308 showed that the binding of the Nse1-Nse3 KITE dimer increases the Nse4 ability to bind SMC5-
309 SMC6 subunits in ATP-free state (Figs. 1B and 3B), suggesting that the KITE binding may

310 shape Nse4 to fit the ATP-free conformation of the SMC5/6 complex. In contrast, the KITE-
311 bound Nse4 linker is barely compatible with the ATP-bound conformation of SMC5/6.
312 Consistent with these notions, 30 amino acid long extension of the Nse4 linker partially relaxed
313 its stiff shape and resulted in a mild drop in the stability of the ATP-free complex (Fig. 4E). In
314 contrary, this extension partially released the ATP-induced constraint in the ATP-bound
315 complex. Further extension of the Nse4 linker decreased the stability of the ATP-free complex
316 further (as the linker became more flexible) to the levels similar to the ATP-bound complex (90
317 amino acid extension fully released ATP-induced constraint; L. Vondrova, unpublished data).
318 Therefore, we suggest that KITE subunits shape the Nse4 linker to fit the ATP-free complex
319 optimally and to facilitate opening of the complex upon ATP binding (Fig. 5). Consistent with
320 this conclusion, the ATP-mediated constraint was partially suppressed upon release of the part
321 of the Nse4 linker from the Nse3 WHB pocket (Fig. 4B; [28, 35]). Altogether, we hypothesize
322 that the Nse4 linker is stiffened upon its KITE binding and transduces a pulling force generated
323 by the binding of ATP to the SMC5-SMC6 heads (Fig. 5B). In consequence, the Nse4-SMC6
324 interface opens and releases the Nse4 constraint. After ATP hydrolysis, the SMC5-ATP-SMC6
325 head dimer is dissolved and Nse4 is reattached to the SMC6 neck.

326 Similarly, it was proposed that binding of the HAWK (Scc3 and Pds5) and Wapl
327 proteins to Scc1 kleisin stiffens its linker region and transduces conformational energy of the
328 ATP-dependent SMC head dimerization to the dissociation of Scc1 from Smc3 [19, 45]. In the
329 absence of the Pds5-Wapl regulators, the cohesin's head movements driven by ATP binding
330 and hydrolysis cannot be effectively coupled to exit gate opening as the Scc1 linker is flexible.
331 Interestingly, the size of the Scc1 linker is much longer (cca 400 amino acids) than the size of
332 the Nse4 linker (and ScpA linker; both having cca 100 amino acids; J. Palecek, unpublished
333 data). Accordingly, the Scc3 HAWK subunit covers only a small part of the Scc1 linker and
334 requires Pds5-Wapl regulators to shape the long Scc1 linker while the KITE subunits are

335 sufficient to shape their short kleisin partners. As mentioned above, the extension of the Nse4
336 linker region suppressed the ATP-induced constraint, suggesting that the short size of the Nse4
337 linker is critical for the dynamics of the SMC5/6 complex. Consistent with this notion, the
338 integration of the 30 amino acid long extension to the genomic copy of the fission yeast Nse4
339 resulted in severe DNA repair phenotypes (L. Vondrova, unpublished data).

340 As the KITE subunits are stable components of the SMC complexes, we assume that the
341 openings of the kleisin-νSMC interfaces are intrinsically coupled to their ATP cycles. It was
342 proposed for the SMC/ScpAB complex that the opening of the kleisin-νSMC interface might
343 be a part of its ATPase cycle generating loops along DNA strands [52, 53]. The SMC5/6 data
344 are also consistent with the above notions as the ATPase activity of the SMC5/6 complex is
345 needed for its topological binding [36]. Interestingly, the Nse1-Nse3 KITE subunits bind DNA
346 and this interaction could anchor or transduce DNA during the loop extrusion mediated by the
347 SMC5/6 complex [37]. In contrast, dissociation of the kleisin-νSMC interface is tightly
348 controlled by Pds5-Wapl regulators and is coupled to cohesin release from chromosome arms.
349 Consistent with these differences, the Scc1-SMC3 fusion is tolerated in cells (as they can
350 release cohesin by other ways; [20, 21, 23, 54]) while the fusion of Nse4 and SMC6 is lethal in
351 fission yeast (L. Vondrova, unpublished data). Our results suggest very similar mechanics
352 shared by the prokaryotic SMC/ScpAB and eukaryotic SMC5/6 complexes (while
353 distinguishing them from cohesin) and further support our recently proposed close evolutionary
354 relationship between these complexes [7].

355 However, there are also apparent differences between the SMC/ScpAB and SMC5/6
356 complexes. Particularly, the Nse1 KITE subunit contains an RING-finger ubiquitin ligase
357 domain which may add a specific regulatory level to SMC5/6 [55]. Interestingly, our *in vitro*
358 and *in vivo* experiments showed an Nse1-dependent Nse4 kleisin ubiquitination of its linker
359 both in *S. pombe* and human proteins ([56]; P. Kolesar, unpublished data). Such a bulky post-

360 translational modification on the Nse4 linker could alter its binding to KITE partners or its
361 stiffness (i.e. alter the SMC5/6 ring opening). Altogether, similarities and differencies between
362 SMC complexes at different levels of their architecture may stay behind their different functions
363 in genomes and remain an intriguing avenue of future research.
364

365 **MATERIAL AND METHODS**

366 **Plasmids**

367 Most of the Y2H constructs were prepared previously: pGBKT7-Nse3(aa1-328), pGADT7-
368 Nse3(aa1-328) and pGBKT7-Nse4(aa1-300) constructs were created in [33], pOAD-Nse1(aa1-
369 232) was created in [35], pGADT7-SMC6 (aa1-1140) was described in [37]. To generate
370 pGBKT7-SMC5(aa1-1076) construct, the yeast *S.pombe* SMC5 cDNA was PCR amplified by
371 oLV511+oLV486 (Supplementary Table 2) and inserted into the *NcoI–SalI* digested pGBKT7
372 by In-Fusion cloning protocol (Clontech). Nse5 was cloned into pGBKT7 vector using *NcoI*
373 and *Sa*lI sites and classical T4 ligase protocol.
374 To create the pGADT7-Nse4(aa1-300)/WT, pGADT7-Nse4(aa1-300)/del87-91 and pGADT7-
375 Nse4(aa1-300)/ext constructs, Nse4 was PCR amplified from the corresponding p416ADH1-
376 Nse4 plasmids (see below) by oLV575+oLV576 and inserted into *NdeI/BamHI* digested
377 pGADT7 by In-Fusion cloning protocol.
378 Multicomponent Y2H system was described in the protocol book series Methods in Molecular
379 Biology [30]. The p416ADH1-Nse1(aa1–232) construct was created previously [35].
380 Construction of p416ADH1-Nse4 (aa1-300), p416ADH1-Nse3(aa1–328)+Nse4(aa1–300) and
381 p416ADH1-Nse3(aa1–328)+Nse4(aa1–300)+Nse1(aa1–232) was described previously ([30,
382 37]; the vector name pPM587 equals to p416ADH1). p416ADH1-Nse4(aa1–300)+Nse1(aa1–
383 232) and p416ADH1-Nse3(aa1–328)+Nse1(aa1–232) were prepared by PCR-amplification of

384 ADH1-Nse1(1-232)-CYC terminator from p416ADH1-Nse1 by KB353+KB354 and its
385 insertion into *KpnI* digested p416ADH1-Nse4 (aa1-300) and p416ADH1-Nse3(aa1–328) by In-
386 Fusion protocol, respectively. The p416ADH1-Nse6(1-522) construct was prepared using PCR-
387 amplification of Nse6 by EB77 + EB78 primers and insertion into *SalI/SpeI* digested
388 p416ADH1 by In-Fusion protocol.
389 To prepare p416ADH1-Nse4-ext, *SalI* restriction site in the p416ADH1 multi-cloning site
390 (MCS) was mutated by site-directed mutagenesis (SDM; see below) with oLV522 + oLV523.
391 Then, *SalI* site was inserted by SDM behind the aa174 with oLV520 + oLV521. This construct
392 was *SalI* digested, $(G_4S)_6$ linker was amplified by oLV579 + oLV580 and inserted using the In-
393 Fusion cloning protocol.
394 Construct for the *S. pombe* genome integration was prepared as follows: 1. Nse4 was cloned
395 within the *BamHI* and *EcoRI* sites of the pSK-ura4 plasmid; 2. genomic sequence downstream
396 of the Nse4 gene was PCR amplified (JP414 and JP415) and inserted to the pGEM-Easy vector
397 (Promega); 3. The *SacI-SalI* fragment of the pSK-Nse4-ura4 plasmid was inserted to the *SacI-*
398 *XhoI* digested pGEM-3'end construct to get the pGEM-Nse4(WT)-ura4 integration plasmid.
399 To create pGEM-Nse4(T65R)-ura4 and pGEM-Nse4(L62C,T65R)-ura4, the Nse4 sequences
400 were PCR amplified from p416ADH1-Nse4 mutant constructs by oLV680 + oLV681
401 (Supplementary Table 2) and inserted into *BamHI-EcoRI* digested pGEM-Nse4(WT)-ura4
402 integration construct by the In-Fusion cloning protocol.
403
404 **Site-directed mutagenesis**
405 The QuikChange Lightning Site-Directed Mutagenesis Kit (Agilent Technologies) was used to
406 create mutations in pGBKT7-SMC5, pGADT7-SMC6, p416ADH1-Nse4, p416ADH1-
407 Nse3+Nse4+Nse1, pGADT7-Nse4, pOAD-Nse1, p416ADH1-Nse1, and pGEM-Nse4. The
408 sequences of primers used for mutagenesis are listed in Supplementary Table 3.

409

410 **Yeast two-hybrid assays**

411 The Gal4-based Y2H system was used to analyze *S. pombe* SMC5/6 complex interactions
412 (detailed protocols are described in the book series Methods in Molecular Biology [30]).
413 Briefly, three plasmids pGBKT7, pGADT7 and p416ADH1 with corresponding proteins were
414 co-transformed into the *Saccharomyces cerevisiae* PJ69–4a strain and selected on SD -Leu, -
415 Trp, -Ura plates. Drop tests were carried out on SD -Leu, -Trp, -Ura, -His (with 0; 0.3; 0.5; 1;
416 2; 3; 4; 5; 10; 15; 20; 30 mM 3-aminotriazole) plates at 28°C. Each combination was co-
417 transformed at least three times and at least three independent drop tests were carried out.

418

419 **Generation of *nse4* mutant strains of *S. pombe***

420 Standard genetic techniques were used for preparation of fission yeast *S. pombe* diploid strain
421 by crossing *ade6-M216* strain with *ade6-M210* [57]. The pGEM-Nse4-ura4 wild-type or mutant
422 integration constructs (digested by *BamHI* and *SalI*) were transformed into the diploid strain
423 and the transformants were selected on –ura –ade plates. Using standard genetic techniques,
424 spores of the *nse4+/nse4-mutant* strains were generated and dissected.

425

426 **PEPSCAN-ELISA**

427 Was performed as described previously [28] with a peptide library (Mimotopes, Australia) of
428 the aa 875-1024 region of the *S. pombe* Smc6 protein (Supplementary Table 1). The library was
429 linked to biotin via an additional peptide spacer of serine–glycine–serine–glycine. The peptides
430 were prebound to ELISA plates (coated with streptavidin) and washed three times with binding
431 buffer (PBS with 0.5% Nonidet NP40). Then, *S. pombe* His-S-Nse4 (aa1-150) protein was
432 added and incubated overnight. Unbound protein was washed (three times) and the peptide-

433 bound Nse4 protein was quantified using anti-His (Sigma H1029, 1:10000) and anti-mouse
434 HRP-conjugated (Sigma A0168, 1:10000) antibodies, respectively. *H. sapiens* His-TRF2 (aa1-
435 542) protein was used as a negative control in the same way [29].
436

437 **FIGURE LEGENDS:**

438 **Figure 1. Nse4 binds neck region of the SMC6 protein.**
439 Peptide library (A) and multi-component yeast two-hybrid systems (B-D) were employed to
440 determine SMC6 region and residues binding to Nse4. (A) Quantification of relative binding of
441 the Nse4(1-150) protein (Nse4; red columns) to the SMC6 synthetic peptides (listed in Suppl.
442 Table S1) using the PEPSCAN-ELISA method. The SMC6(aa960-984) peptide exhibits the
443 highest affinity and specificity to Nse4. Results show mean $\pm$ SEM of 3 independent
444 measurements. His-TRF2 protein (TRF2; white columns) was used in the control experiment.
445 (B-D) Impact of mutations on the stability of the following SMC6 complexes was tested:
446 SMC6-Nse4-Nse3-Nse1 (B), SMC6-Nse4-SMC5 (C) and SMC6-Nse5-Nse6 (D). Schematic
447 representation of the complexes is at the right side of each panel. (B) The full-length hybrid
448 SMC6 (fused to Gal4AD domain) and Nse4 (fused to Gal4BD domain) constructs were co-
449 transformed together with Nse1+Nse3 plasmid (p416ADH1 vector backbone) into *S. cerevisiae*
450 PJ69 cells. Formation and stability of the SMC6-Nse4-Nse3-Nse1 complex was scored by
451 growth of yeast PJ69 transformants on plates without leucine, tryptophan, uracil and histidine,
452 containing 0.3 mM 3-Amino-1,2,4-triazole (-L,T,U,H, 0.3AT panel). The L964A, L965A,
453 L968A, E969A, L972A and R975A mutations reduce stability of the SMC6 complexes. (C)
454 Similarly, the full-length hybrid SMC6 (fused to Gal4AD domain) and SMC5 (fused to Gal4BD
455 domain) were co-transformed together with non-hybrid Nse4 full-length construct (p416ADH1
456 vector) and stability of the SMC5-Nse4-SMC6 complex was scored on plates containing 0.5
457 mM 3-Amino-1,2,4-triazole (-L,T,U,H, 0.5AT panel). The L964A, L965A, L968A, E969A,

458 L972A and R975A mutations reduce stability of the SMC6 complexes. (D) In the control
459 experiment, the same mutations were tested in the SMC6-Nse5-Nse6 complex (constituted of
460 the full-length Gal4AD-SMC6, Gal4BD-Nse5 and non-hybrid Nse6). Stability of the SMC6-
461 Nse5-Nse6 complex was scored on plates containing 3 mM 3-Amino-1,2,4-triazole (-L,T,U,H,
462 3AT panel). The L964A, L968A and E969A mutations affect all SMC6 complexes (B-D) while
463 L965A, L972A and R975A mutations reduce only stability of SMC6-Nse4 complexes (B and
464 C), suggesting that the highly conserved L965, L972 and L975 residues (Suppl. Fig. S1B) are
465 specifically required for the SMC6 interaction with Nse4. Wild-type (WT) or mutant versions
466 of SMC6 are labelled in blue below the panels; "-", control empty vector; "+", co-transformed
467 construct (as labelled at the left side). Growth of the transformants was verified on control plates
468 without leucine, tryptophan and uracil (-L,T,U). All mY2H tests were repeated at least 3 times.
469

470 **Figure 2. Binding of the Nse4 helix H3 to SMC6 is essential for yeast viability.**
471 Identification of the SMC6-binding residues within the Nse4 helix H3 region (aa62-68). (A)
472 Stability of the SMC5-Nse4-SMC6 complex was scored by 3Y2H on plates containing 0.5 mM
473 3-Amino-1,2,4-triazole (-L,T,U,H, 0.5 AT panel; further details as in Fig. 1). The Nse4/L62C,
474 K64C, T65R, D67C, and L68C mutations reduce stability of the SMC6 complexes. In the
475 control experiment (B), the same mutations were tested for the Nse4-Nse3 interaction in the
476 classical Y2H system (constituted of the full-length Gal4AD-Nse4 and Gal4BD-Nse3).
477 Interactions were scored on plates containing 10 mM 3-Amino-1,2,4-triazole (-L,T,U,H, 10AT
478 panel). The K64C and D67C mutations affect all Nse4 complexes (A and B). Intact L62, T65
479 and L68 Nse4 residues are required specifically for binding to SMC6. Wild-type (WT) or
480 mutant versions of Nse4 are labelled in violet below the panels (further details as in Fig. 1). (C)
481 Alignment of the Nse4 helix H3 (of the N-terminal HTH domain). The orthologs are from
482 *Schizosaccharomyces pombe* (*S.p.*), *Aspergillus nidulans* (*A.n.*), *Aspergillus clavatus* (*A.c.*),

483 *Danio rerio* (*D.r.*), *Xenopus laevis* (*X.l.*), *Ornithorhynchus anatinus* (*O.a.*), *Monodelphis*
484 *domestica* (*M.d.*), *Loxodonta africana* (*L.a.*), *Dasypus novemcinctus* (*D.n.*), *Mus musculus*
485 (*M.m.*), *Homo sapiens* (*H.s.*). Note that there are two Nse4 genes in the placental mammals
486 denoted as A and B. "+", mutation not affecting Nse4 interactions; "-", mutation disrupting all
487 Nse4 complexes; red minus, mutation specifically disrupting the Nse4-SMC6 interaction.
488 Amino acid shading represents following conserved amino acids: *dark green*, hydrophobic and
489 aromatic; *light green*, polar; *pink*, basic; *blue*, acidic. (D) Tetrad dissection analysis of yeast *S.*
490 *pombe* diploid strains *nse4*$^{+}$*/nse4-T65R* (top) and *nse4*$^{+}$*/nse4-L62C, T65R* (bottom). The *nse4-*
491 *T65RC* and *nse4-L62C, T65R* mutations are lethal, suggesting essential role of the Nse4–SMC6
492 interaction.
493
494 **Figure 3. A role of Nse4 and ATP molecules in bridging of SMC5-SMC6.**
495 (A) Nse4 is essential for the bridging of the hybrid SMC5-SMC6 constructs (columns 1-4). The
496 SMC5/E995 conserved residue was mutated to glutamine (EQ) to inhibit ATP hydrolysis. The
497 ATP retention has only mild additive effect on the stability of the SMC5-Nse4-SMC6 complex
498 (scored on plates containing increasing concentrations of 3-Amino-1,2,4-triazole). The Nse4
499 mutations affected the stability of the wild-type SMC5 complexes more dramatically than the
500 stability of the SMC5/E995Q mutant complexes (compare odd and even columns). Wild-type
501 (WT) or E995Q (EQ) mutant versions of SMC5 are labelled in grey below the panels (further
502 details as in Figs. 1 and 2). (B) Addition of the Nse1 and Nse3 KITE proteins to the above
503 SMC5/SMC6/Nse4 system stabilizes the SMC5-Nse4-SMC6 bridge. Although the KITE
504 proteins stabilize the ATP-free SMC5-Nse4-SMC6 complex (columns 1 and 3), they destabilize
505 ATP-bound complex (columns 2 and 4). The Nse4 mutations decrease stability of the ATP-free
506 SMC5-SMC6-Nse4-Nse3-Nse1 complex gradually (columns 5, 7, 9 and 11) while the stability

507 of the ATP-bound complexes drops first (columns 6, 8, and 10) and then it recovers in the
508 L62C, T65R double mutant (column 12).
509
510 **Figure 4. KITE proteins constrain Nse4 kleisin linker.**
511 (A) The Nse1-Nse3-Nse4 subcomplex is held by mutual interactions between its subunits. The
512 Nse4/del87-91 (del) deletion disturbs the Nse3-Nse4 binary interaction (columns 3 and 4) and
513 the Nse1/Q18A, M21A (QM) double mutation abrogates the Nse1-Nse3 binary interaction
514 (columns 9 and 10), but they do not alter stability of the Nse1-Nse3-Nse4 trimer individually
515 (columns 6 and 7). However, combination of these two mutations reduces the stability of Nse1-
516 Nse3-Nse4 significantly (column 8). (B) The combination of the Nse4/del87-91 and
517 Nse1/Q18A, M21A mutations compromises stability of the wild-type SMC5-SMC6-Nse4-
518 Nse3-Nse1 complex (compare columns 6 and 8), but increases the stability of the ATP-bound
519 complex (compare columns 7 and 9). Notably, there is no difference between stability of ATP-
520 free and ATP-bound complexes (compare columns 8 and 9), suggesting that the binding of
521 KITE proteins to Nse4 destabilizes ATP-bound complexes. Furthermore, the Nse4/del87-91
522 mutation alone also partially supresses the instability of the ATP-bound complex (column 11),
523 suggesting that the binding of Nse3 to Nse4 linker constrains the linker. (C) Schematic of the
524 Nse4 regions with their binding partners (depicted above). The 30 amino acid extension is
525 inserted at the end of the linker. (D) The 30 amino acid extension (ext) was tested in control
526 experiments for the stability of either Nse3-Nse4 binary interaction (column 4) or Nse1-Nse3-
527 Nse4 trimer (column 6). (E) The extension of the linker results in partial relieve of the ATP-
528 induced tension in the SMC5/E995Q complex (compare columns 5 and 6).
529
530 **Figure 5. SMC5/6 ATPase cycle model.**

531 Binding of ATP to the SMC heads leads to their dimerization and changes their mutual position
532 (states 1-3). (A) Nse4 bridges SMC heads and supports the ATP-mediated head dimerization in
533 the absence of the KITE proteins. (B) Addition of the Nse1 and Nse3 KITE proteins stabilizes
534 the otherwise flexible Nse4 linker in a position that is favoured in the ATP-free complex (state
535 B1). In contrast, the KITE-bound Nse4 linker shape is adverse in the ATP-bound complex (state
536 B3). The stiff KITE-bound Nse4 linker transduces a pulling force generated by the binding of
537 ATP to the SMC5-SMC6 heads and forces the Nse4-SMC6 interface apart (state B3). After
538 ATP hydrolysis, the SMC5-SMC6 head dimer is dissolved and Nse4 is reattached to the SMC6
539 arm (state B4).
540

541 **SUPPORTING INFORMATION**

542 **Supplementary Figure S1. Nse4 binds neck region of SMC6.**
543 Peptide library (A) and multi-component yeast two-hybrid systems (C-E) were employed to
544 determine the SMC6 region and residues binding to Nse4. (A) Quantification of relative binding
545 of the Nse4(1-150) protein (Nse4; red columns) to the SMC6 synthetic peptides (listed in
546 Supplementary Table 1) using the PEPSCAN-ELISA method. The SMC6(aa960-984) peptide
547 exhibits the highest affinity and specificity to Nse4. Results show mean ± SEM of 3 independent
548 measurements. His-TRF2 protein (TRF2; white column) was used in the control experiment.
549 (B) Alignment of the C-terminal SMC6 neck region. The orthologs are from
550 *Schizosaccharomyces pombe* (*S.p.*), *Aspergillus nidulans* (*A.n.*), *Aspergillus clavatus* (*A.c.*), *S.*
551 *cerevisiae* (*S.c.*), *Danio rerio* (*D.r.*), *Xenopus laevis* (*X.l.*), *Ornithorhynchus anatinus* (*O.a.*),
552 *Loxodonta africana* (*L.a.*), *Monodelphis domestica* (*M.d.*), *Dasypus novemcinctus* (*D.n.*), *Mus*
553 *musculus* (*M.m.*), *Homo sapiens* (*H.s.*). "+", mutation not affecting SMC6 interactions; "-",
554 mutation disrupting all SMC6 complexes; red minus, mutation specifically disrupting the Nse4-
555 SMC6 interaction. Amino acid shading represents following conserved amino acids: *dark*

556 *green*, hydrophobic and aromatic; *light green*, polar; *pink*, basic. (C-E) To identify Nse4-
557 binding residues, stability of the following SMC6 mutant complexes was tested: SMC6-Nse4-
558 Nse3-Nse1 (C), SMC6-Nse4-SMC5 (D) and SMC6-Nse5-Nse6 (E). (C) The full-length hybrid
559 SMC6 (fused to Gal4AD domain) and Nse4 (fused to Gal4BD domain) were co-transformed
560 together with Nse1-Nse3 construct (p416ADH1 vector) into PJ69 cells. Formation and stability
561 of the SMC6-Nse4-Nse3-Nse1 complex was scored by growth of yeast PJ69 transformants on
562 plates without Leu, Trp, Ura and His, containing 0.3 mM 3-Amino-1,2,4-triazole (-L,T,U,H,
563 0.3AT panel). (D) Similarly, the full-length SMC6 (fused to Gal4AD domain) and SMC5 (fused
564 to Gal4BD domain) were co-transformed together with Nse4 full-length construct (in
565 p416ADH1 vector) and stability of the SMC5-Nse4-SMC6 complex was scored on plates
566 containing 0.5 mM 3-Amino-1,2,4-triazole (-L,T,U,H, 0.5AT panel). The L964A, L965A,
567 L968A, E969A, L972A and R975A mutations reduce stability of the SMC6-Nse4 complexes
568 (C and D). (E) In the control experiment, the same mutations were introduced to SMC6-Nse5-
569 Nse6 complex (constituted of the full-length Gal4AD-SMC6, Gal4BD-Nse5 and non-hybrid
570 Nse6). Stability of the SMC6-Nse5-Nse6 complex was scored on plates containing 3 mM 3-
571 Amino-1,2,4-triazole (-L,T,U,H, 3AT panel). The L964A, L968A and E969A mutations
572 affected all SMC6 complexes (C-E). In contrast, the highly conserved L965, L972 and L975
573 SMC6 residues (panel B) were required specifically for binding to Nse4. Wild-type (WT) or
574 mutant versions of SMC6 are labelled in blue below the panels; "-", control empty vector; "+",
575 co-transformed construct (as labelled at the left side). Growth of the transformants was verified
576 on control plates without leucine, tryptophan and uracil (-L,T,U). All Y2H tests were repeated
577 at least 3 times.
578
579 **Supplementary Figure S2. The SMC5-SMC6-Nse4-Nse3-Nse1 instability is dependent on**
580 **the ATP binding and SMC5-SMC6 head dimerization.**

581 (A-B) Alignment of the conserved SMC head motifs mutated in the SMC5 and SMC6
582 constructs. Arrows point to the positions of the fission yeast SMC5/K57I mutation in the
583 Walker A motif disturbing ATP binding (A), the SMC6/S1045R mutation in the Signature motif
584 abrogating ATP-mediated SMC5-SMC6 head dimerization (B), and the SMC5/E995Q
585 mutation in the Walker B motif inhibiting ATP hydrolysis (B). The SMC homologs are from
586 *Bacilus subtilis* (*B.s.*), *Schizosaccharomyces pombe* (*S.p.*), *Homo sapiens* (*H.s.*). Amino acid
587 shading as in Fig. S1. (C) Stability of the SMC5-SMC6-Nse4 (columns 1-6) and SMC5-SMC6-
588 Nse4-Nse3-Nse1 (columns 7-12) complexes was scored on plates containing increasing
589 concentrations of 3-Amino-1,2,4-triazole (AT). The SMC5/K57I (KI) mutation disturbing ATP
590 binding and SMC6/S1045R (SR) mutation abrogating ATP-mediated SMC5-SMC6 head
591 dimerization have no effect on the SMC5-SMC6-Nse4 complex irrespective of the
592 SMC5/E995Q mutation (columns 3-6). In contrast, destabilizing effect of the SMC5/E995Q
593 mutation was fully supressed by both KI and SR mutations in the SMC5-SMC6-Nse4-Nse3-
594 Nse1 complex (compare columns 8, 10 and 12), suggesting that the instability is caused by the
595 ATP binding and ATP-mediated head dimerization. Mutant versions of SMC5 and SMC6 are
596 labelled in grey and blue, respectively (further details as in Fig. S1).

597

598 **Supplementary Table 1: SMC6(aa875-1024) peptide library**

599

600 **Supplementary Table 2: Primers used for PCR**

601

602 **Supplementary Table 3: Primers used for site-directed mutagenesis**

603

604 **ACKNOWLEDGMENTS**

605 We thank C. Hofr for providing the purified His-hTRF2 protein for the ELISA assays.
606 We are grateful to A.R. Lehmann and K. Zabrady for the critical reading of our manuscript.

607

608 **REFERENCES**

609 1. Schwarzer W, Abdennur N, Goloborodko A, Pekowska A, Fudenberg G, Loe-Mie Y,
610 et al. Two independent modes of chromatin organization revealed by cohesin removal.
611 Nature. 2017; 551(7678):51-6. Epub 2017/09/27. doi: 10.1038/nature24281. PubMed PMID:
612 29094699; PubMed Central PMCID: PMCPMC5687303.
613 2. Kschonsak M, Haering CH. Shaping mitotic chromosomes: From classical concepts to
614 molecular mechanisms. Bioessays. 2015;37(7):755-66. doi: 10.1002/bies.201500020.
615 PubMed PMID: 25988527; PubMed Central PMCID: PMCPMC4683672.
616 3. Aragon L. The Smc5/6 Complex: New and Old Functions of the Enigmatic Long-
617 Distance Relative. In: Bonini NM, editor. Annual Review of Genetics, Vol 52. Annual
618 Review of Genetics. 52. Palo Alto: Annual Reviews; 2018. p. 89-107.
619 4. Palecek JJ. SMC5/6: Multifunctional Player in Replication. Genes. 2019;10(1):E7.
620 doi: 10.3390/genes10010007. PubMed PMID: WOS:000459743800007.
621 5. Bürmann F, Gruber S. SMC condensin: promoting cohesion of replicon arms. Nat
622 Struct Mol Biol. 2015;22(9):653-5. doi: 10.1038/nsmb.3082. PubMed PMID: 26333713.
623 6. van der Crabben SN, Hennus MP, McGregor GA, Ritter DI, Nagamani SCS, Wells
624 OS, et al. Destabilized SMC5/6 complex leads to chromosome breakage syndrome with
625 severe lung disease. Journal of Clinical Investigation. 2016;126(8):2881-92. doi:
626 10.1172/jci82890. PubMed PMID: WOS:000381943000013.
627 7. Palecek JJ, Gruber S. Kite Proteins: a Superfamily of SMC/Kleisin Partners
628 Conserved Across Bacteria, Archaea, and Eukaryotes. Structure. 2015;23(12):2183-90. doi:
629 10.1016/j.str.2015.10.004. PubMed PMID: WOS:000366171500001.

630 8. Wells JN, Gligoris TG, Nasmyth KA, Marsh JA. Evolution of condensin and cohesin
631 complexes driven by replacement of Kite by Hawk proteins. Curr Biol. 2017;27(1):R17-R8.
632 doi: 10.1016/j.cub.2016.11.050. PubMed PMID: 28073014; PubMed Central PMCID:
633 PMCPMC5228436.
634 9. Burmann F, Basfeld A, Nunez RV, Diebold-Durand ML, Wilhelm L, Gruber S. Tuned
635 SMC Arms Drive Chromosomal Loading of Prokaryotic Condensin. Molecular Cell.
636 2017;65(5):861-+. doi: 10.1016/j.molcel.2017.01.026. PubMed PMID:
637 WOS:000396431700010.
638 10. Diebold-Durand ML, Lee H, Ruiz Avila LB, Noh H, Shin HC, Im H, et al. Structure
639 of Full-Length SMC and Rearrangements Required for Chromosome Organization. Mol Cell.
640 2017;67(2):334-47.e5. Epub 2017/07/06. doi: 10.1016/j.molcel.2017.06.010. PubMed PMID:
641 28689660; PubMed Central PMCID: PMCPMC5526789.
642 11. Nasmyth K, Haering CH. The structure and function of SMC and kleisin complexes.
643 Annu Rev Biochem. 2005;74:595-648.
644 12. Hassler M, Shaltiel IA, Haering CH. Towards a Unified Model of SMC Complex
645 Function. Curr Biol. 2018;28(21):R1266-R81. doi: 10.1016/j.cub.2018.08.034. PubMed
646 PMID: 30399354.
647 13. Gligoris T, Löwe J. Structural Insights into Ring Formation of Cohesin and Related
648 Smc Complexes. Trends Cell Biol. 2016;26(9):680-93. Epub 2016/04/28. doi:
649 10.1016/j.tcb.2016.04.002. PubMed PMID: 27134029; PubMed Central PMCID:
650 PMCPMC4989898.
651 14. Lammens A, Schele A, Hopfner KP. Structural biochemistry of ATP-driven
652 dimerization and DNA-stimulated activation of SMC ATPases. Curr Biol. 2004;14(19):1778-
653 82.

654 15. Arumugam P, Gruber S, Tanaka K, Haering CH, Mechtler K, Nasmyth K. ATP
655 hydrolysis is required for cohesin's association with chromosomes. Curr Biol.
656 2003;13(22):1941-53.
657 16. Bürmann F, Shin HC, Basquin J, Soh YM, Giménez-Oya V, Kim YG, et al. An
658 asymmetric SMC-kleisin bridge in prokaryotic condensin. Nat Struct Mol Biol.
659 2013;20(3):371-9. Epub 2013/01/27. doi: 10.1038/nsmb.2488. PubMed PMID: 23353789.
660 17. Gligoris TG, Scheinost JC, Bürmann F, Petela N, Chan KL, Uluocak P, et al. Closing
661 the cohesin ring: structure and function of its Smc3-kleisin interface. Science.
662 2014;346(6212):963-7. doi: 10.1126/science.1256917. PubMed PMID: 25414305; PubMed
663 Central PMCID: PMCPMC4300515.
664 18. Zawadzka K, Zawadzki P, Baker R, Rajasekar KV, Wagner F, Sherratt DJ, et al.
665 MukB ATPases are regulated independently by the N- and C-terminal domains of MukF
666 kleisin. Elife. 2018;7. Epub 2018/01/11. doi: 10.7554/eLife.31522. PubMed PMID:
667 29323635; PubMed Central PMCID: PMCPMC5812716.
668 19. Murayama Y, Uhlmann F. DNA Entry into and Exit out of the Cohesin Ring by an
669 Interlocking Gate Mechanism. Cell. 2015;163(7):1628-40. doi: 10.1016/j.cell.2015.11.030.
670 PubMed PMID: 26687354; PubMed Central PMCID: PMCPMC4701713.
671 20. Beckouët F, Srinivasan M, Roig MB, Chan KL, Scheinost JC, Batty P, et al. Releasing
672 Activity Disengages Cohesin's Smc3/Scc1 Interface in a Process Blocked by Acetylation. Mol
673 Cell. 2016;61(4):563-74. doi: 10.1016/j.molcel.2016.01.026. PubMed PMID: 26895425;
674 PubMed Central PMCID: PMCPMC4769318.
675 21. Buheitel J, Stemmann O. Prophase pathway-dependent removal of cohesin from
676 human chromosomes requires opening of the Smc3-Scc1 gate. EMBO J. 2013;32(5):666-76.
677 Epub 2013/01/29. doi: 10.1038/emboj.2013.7. PubMed PMID: 23361318; PubMed Central
678 PMCID: PMCPMC3590994.

679 22. Eichinger CS, Kurze A, Oliveira RA, Nasmyth K. Disengaging the Smc3/kleisin
680 interface releases cohesin from Drosophila chromosomes during interphase and mitosis.
681 EMBO J. 2013;32(5):656-65. Epub 2013/01/22. doi: 10.1038/emboj.2012.346. PubMed
682 PMID: 23340528; PubMed Central PMCID: PMCPMC3590983.
683 23. Chan KL, Roig MB, Hu B, Beckouët F, Metson J, Nasmyth K. Cohesin's DNA exit
684 gate is distinct from its entrance gate and is regulated by acetylation. Cell. 2012;150(5):961-
685 74. Epub 2012/08/14. doi: 10.1016/j.cell.2012.07.028. PubMed PMID: 22901742; PubMed
686 Central PMCID: PMCPMC3485559.
687 24. Elbatsh AMO, Haarhuis JHI, Petela N, Chapard C, Fish A, Celie PH, et al. Cohesin
688 Releases DNA through Asymmetric ATPase-Driven Ring Opening. Mol Cell.
689 2016;61(4):575-88. doi: 10.1016/j.molcel.2016.01.025. PubMed PMID: 26895426; PubMed
690 Central PMCID: PMCPMC4769319.
691 25. Minnen A, Bürmann F, Wilhelm L, Anchimiuk A, Diebold-Durand ML, Gruber S.
692 Control of Smc Coiled Coil Architecture by the ATPase Heads Facilitates Targeting to
693 Chromosomal ParB/parS and Release onto Flanking DNA. Cell Rep. 2016;14(8):2003-16.
694 Epub 2016/02/18. doi: 10.1016/j.celrep.2016.01.066. PubMed PMID: 26904953; PubMed
695 Central PMCID: PMCPMC4785775.
696 26. Kamada K, Su'etsugu M, Takada H, Miyata M, Hirano T. Overall Shapes of the SMC-
697 ScpAB Complex Are Determined by Balance between Constraint and Relaxation of Its
698 Structural Parts. Structure. 2017;25(4):603-16.e4. Epub 2017/03/09. doi:
699 10.1016/j.str.2017.02.008. PubMed PMID: 28286005.
700 27. Palecek J, Vidot S, Feng M, Doherty AJ, Lehmann AR. The SMC5-6 DNA repair
701 complex: Bridging of the SMC5-6 heads by the Kleisin, NSE4, and non-Kleisin subunits. J
702 Biol Chem. 2006;281:36952-9. PubMed PMID: 17005570.

703 28. Guerineau M, Kriz Z, Kozakova L, Bednarova K, Janos P, Palecek J. Analysis of the
704 Nse3/MAGE-Binding Domain of the Nse4/EID Family Proteins. PLoS One.
705 2012;7(4):e35813.
706 29. Nečasová I, Janoušková E, Klumpler T, Hofr C. Basic domain of telomere guardian
707 TRF2 reduces D-loop unwinding whereas Rap1 restores it. Nucleic Acids Research.
708 2017;45(21):12170-80. doi: 10.1093/nar/gkx812.
709 30. Paleček JJ, Vondrová L, Zábrady K, Otočka J. Multicomponent Yeast Two-Hybrid
710 System: Applications to Study Protein-Protein Interactions in SMC Complexes. Methods Mol
711 Biol. 2019;2004:79-90. doi: 10.1007/978-1-4939-9520-2_7. PubMed PMID: 31147911.
712 31. Duan X, Yang Y, Chen YH, Arenz J, Rangi GK, Zhao X, et al. Architecture of the
713 Smc5/6 Complex of Saccharomyces cerevisiae Reveals a Unique Interaction between the
714 Nse5-6 Subcomplex and the Hinge Regions of Smc5 and Smc6. J Biol Chem.
715 2009;284(13):8507-15. PubMed PMID: 19141609.
716 32. Diaz M, Pecinkova P, Nowicka A, Baroux C, Sakamoto T, Gandha PY, et al. SMC5/6
717 Complex Subunit NSE4A is Involved in DNA Damage Repair and Seed Development in
718 Arabidopsis. Plant Cell. 2019. Epub 2019/04/29. doi: 10.1105/tpc.18.00043. PubMed PMID:
719 31036599.
720 33. Sergeant J, Taylor E, Palecek J, Fousteri M, Andrews E, Sweeney S, et al.
721 Composition and architecture of the Schizosaccharomyces pombe Rad18 (Smc5-6) complex.
722 Mol Cell Biol. 2005;25:172-84.
723 34. Hassler M, Shaltiel IA, Kschonsak M, Simon B, Merkel F, Thärichen L, et al.
724 Structural Basis of an Asymmetric Condensin ATPase Cycle. Mol Cell. 2019;74(6):1175-
725 88.e9. doi: 10.1016/j.molcel.2019.03.037. PubMed PMID: 31226277.
726 35. Hudson JJR, Bednarova K, Kozakova L, Liao C, Guerineau M, Colnaghi R, et al.
727 Interactions between the Nse3 and Nse4 Components of the SMC5-6 Complex Identify

728 Evolutionarily Conserved Interactions between MAGE and EID Families. Plos One.
729 2011;6(2). doi: 10.1371/journal.pone.0017270. PubMed PMID: WOS:000287764100039.
730 36. Kanno T, Berta DG, Sjögren C. The Smc5/6 Complex Is an ATP-Dependent
731 Intermolecular DNA Linker. Cell Rep. 2015;12(9):1471-82. doi:
732 10.1016/j.celrep.2015.07.048. PubMed PMID: 26299966.
733 37. Zabrady K, Adamus M, Vondrova L, Liao C, Skoupilova H, Novakova M, et al.
734 Chromatin association of the SMC5/6 complex is dependent on binding of its NSE3 subunit
735 to DNA. Nucleic Acids Res. 2016;44(3):1064-79. doi: 10.1093/nar/gkv1021. PubMed PMID:
736 26446992; PubMed Central PMCID: PMCPMC4756808.
737 38. Fousteri MI, Lehmann AR. A novel SMC protein complex in Schizosaccharomyces
738 pombe contains the Rad18 DNA repair protein. EMBO J. 2000;19(7):1691-702.
739 39. Kamada K, Miyata M, Hirano T. Molecular basis of SMC ATPase activation: role of
740 internal structural changes of the regulatory subcomplex ScpAB. Structure. 2013;21(4):581-
741 94. doi: 10.1016/j.str.2013.02.016. PubMed PMID: 23541893.
742 40. Woo JS, Lim JH, Shin HC, Suh MK, Ku B, Lee KH, et al. Structural studies of a
743 bacterial condensin complex reveal ATP-dependent disruption of intersubunit interactions.
744 Cell. 2009;136(1):85-96.
745 41. Gloyd M, Ghirlando R, Guarné A. The role of MukE in assembling a functional
746 MukBEF complex. J Mol Biol. 2011;412(4):578-90. Epub 2011/08/10. doi:
747 10.1016/j.jmb.2011.08.009. PubMed PMID: 21855551; PubMed Central PMCID:
748 PMCPMC3482342.
749 42. Pebernard S, Wohlschlegel J, McDonald WH, Yates JR, 3rd, Boddy MN. The Nse5-
750 Nse6 dimer mediates DNA repair roles of the Smc5-Smc6 complex. Mol Cell Biol.
751 2006;26(5):1617-30. PubMed PMID: 16478984.

752 43. Ganji M, Shaltiel IA, Bisht S, Kim E, Kalichava A, Haering CH, et al. Real-time
753 imaging of DNA loop extrusion by condensin. Science. 2018. Epub 2018/02/22. doi:
754 10.1126/science.aar7831. PubMed PMID: 29472443.
755 44. Hirano M, Hirano T. Positive and negative regulation of SMC-DNA interactions by
756 ATP and accessory proteins. Embo J. 2004;23(13):2664-73. Epub 004 Jun 3.
757 45. Ouyang Z, Yu H. Releasing the cohesin ring: A rigid scaffold model for opening the
758 DNA exit gate by Pds5 and Wapl. Bioessays. 2017;39(4). Epub 2017/02/21. doi:
759 10.1002/bies.201600207. PubMed PMID: 28220956.
760 46. Soh YM, Bürmann F, Shin HC, Oda T, Jin KS, Toseland CP, et al. Molecular basis for
761 SMC rod formation and its dissolution upon DNA binding. Mol Cell. 2015;57(2):290-303.
762 doi: 10.1016/j.molcel.2014.11.023. PubMed PMID: 25557547; PubMed Central PMCID:
763 PMCPMC4306524.
764 47. Chapard C, Jones R, van Oepen T, Scheinost JC, Nasmyth K. Sister DNA Entrapment
765 between Juxtaposed Smc Heads and Kleisin of the Cohesin Complex. Mol Cell.
766 2019;75(2):224-37.e5. Epub 2019/06/11. doi: 10.1016/j.molcel.2019.05.023. PubMed PMID:
767 31201089; PubMed Central PMCID: PMCPMC6675936.
768 48. Bürmann F, Lee BG, Than T, Sinn L, O'Reilly FJ, Yatskevich S, et al. A folded
769 conformation of MukBEF and cohesin. Nat Struct Mol Biol. 2019;26(3):227-36. Epub
770 2019/03/04. doi: 10.1038/s41594-019-0196-z. PubMed PMID: 30833788; PubMed Central
771 PMCID: PMCPMC6433275.
772 49. Hara K, Zheng G, Qu Q, Liu H, Ouyang Z, Chen Z, et al. Structure of cohesin
773 subcomplex pinpoints direct shugoshin-Wapl antagonism in centromeric cohesion. Nat Struct
774 Mol Biol. 2014;21(10):864-70. Epub 2014/08/31. doi: 10.1038/nsmb.2880. PubMed PMID:
775 25173175; PubMed Central PMCID: PMCPMC4190070.

776 50. Muir KW, Kschonsak M, Li Y, Metz J, Haering CH, Panne D. Structure of the Pds5-
777 Scc1 Complex and Implications for Cohesin Function. Cell Rep. 2016;14(9):2116-26. Epub
778 2016/02/25. doi: 10.1016/j.celrep.2016.01.078. PubMed PMID: 26923589.
779 51. Lee BG, Roig MB, Jansma M, Petela N, Metson J, Nasmyth K, et al. Crystal Structure
780 of the Cohesin Gatekeeper Pds5 and in Complex with Kleisin Scc1. Cell Rep.
781 2016;14(9):2108-15. Epub 2016/02/25. doi: 10.1016/j.celrep.2016.02.020. PubMed PMID:
782 26923598; PubMed Central PMCID: PMCPMC4793087.
783 52. Baxter J, Oliver AW, Schalbetter SA. Are SMC Complexes Loop Extruding Factors?
784 Linking Theory With Fact. Bioessays. 2019;41(1):e1800182. Epub 2018/12/03. doi:
785 10.1002/bies.201800182. PubMed PMID: 30506702.
786 53. Vazquez Nunez R, Ruiz Avila LB, Gruber S. Transient DNA Occupancy of the SMC
787 Interarm Space in Prokaryotic Condensin. Mol Cell. 2019;75(2):209-23.e6. Epub 2019/06/11.
788 doi: 10.1016/j.molcel.2019.05.001. PubMed PMID: 31201090.
789 54. Gruber S, Arumugam P, Katou Y, Kuglitsch D, Helmhart W, Shirahige K, et al.
790 Evidence that loading of cohesin onto chromosomes involves opening of its SMC hinge. Cell.
791 2006;127(3):523-37.
792 55. McDonald WH, Pavlova Y, Yates JR, Boddy MN. Novel essential DNA repair
793 proteins Nse1 and Nse2 are subunits of the fission yeast Smc5-Smc6 complex. J Biol Chem.
794 2003;278(46):45460-7. doi: 10.1074/jbc.M308828200. PubMed PMID: 12966087.
795 56. Kozakova L, Vondrova L, Stejskal K, Charalabous P, Kolesar P, Lehmann AR, et al.
796 The melanoma-associated antigen 1 (MAGEA1) protein stimulates the E3 ubiquitin-ligase
797 activity of TRIM31 within a TRIM31-MAGEA1-NSE4 complex. Cell Cycle.
798 2015;14(6):920-30. doi: 10.1080/15384101.2014.1000112. PubMed PMID:
799 WOS:000351598200022.

800 57. Moreno S, Klar A, Nurse P. Molecular genetic analysis of fission yeast
801 Schizosaccharomyces pombe. Methods Enzymol. 1991;194:795-823. doi: 10.1016/0076-
802 6879(91)94059-l. PubMed PMID: 2005825.

803

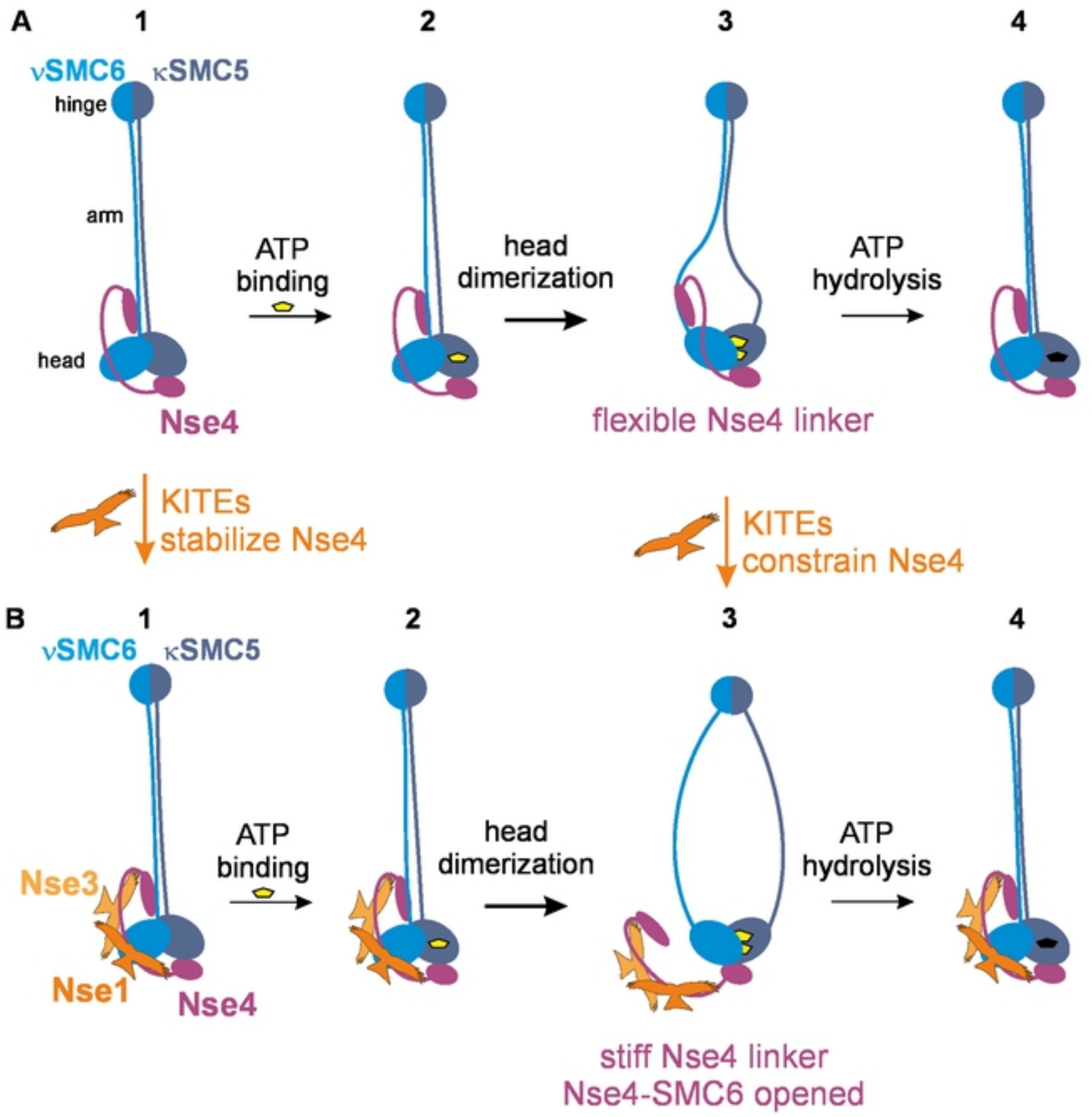
A
1
2
3
4
νSMC6
κSMC5
hinge
arm
head
ATP binding
head dimerization
ATP hydrolysis
Nse4
flexible Nse4 linker
KITEs stabilize Nse4
KITEs constrain Nse4
B
1
2
3
4
νSMC6
κSMC5
Nse3
Nse1
Nse4
ATP binding
head dimerization
ATP hydrolysis
stiff Nse4 linker
Nse4-SMC6 opened

Figure 5

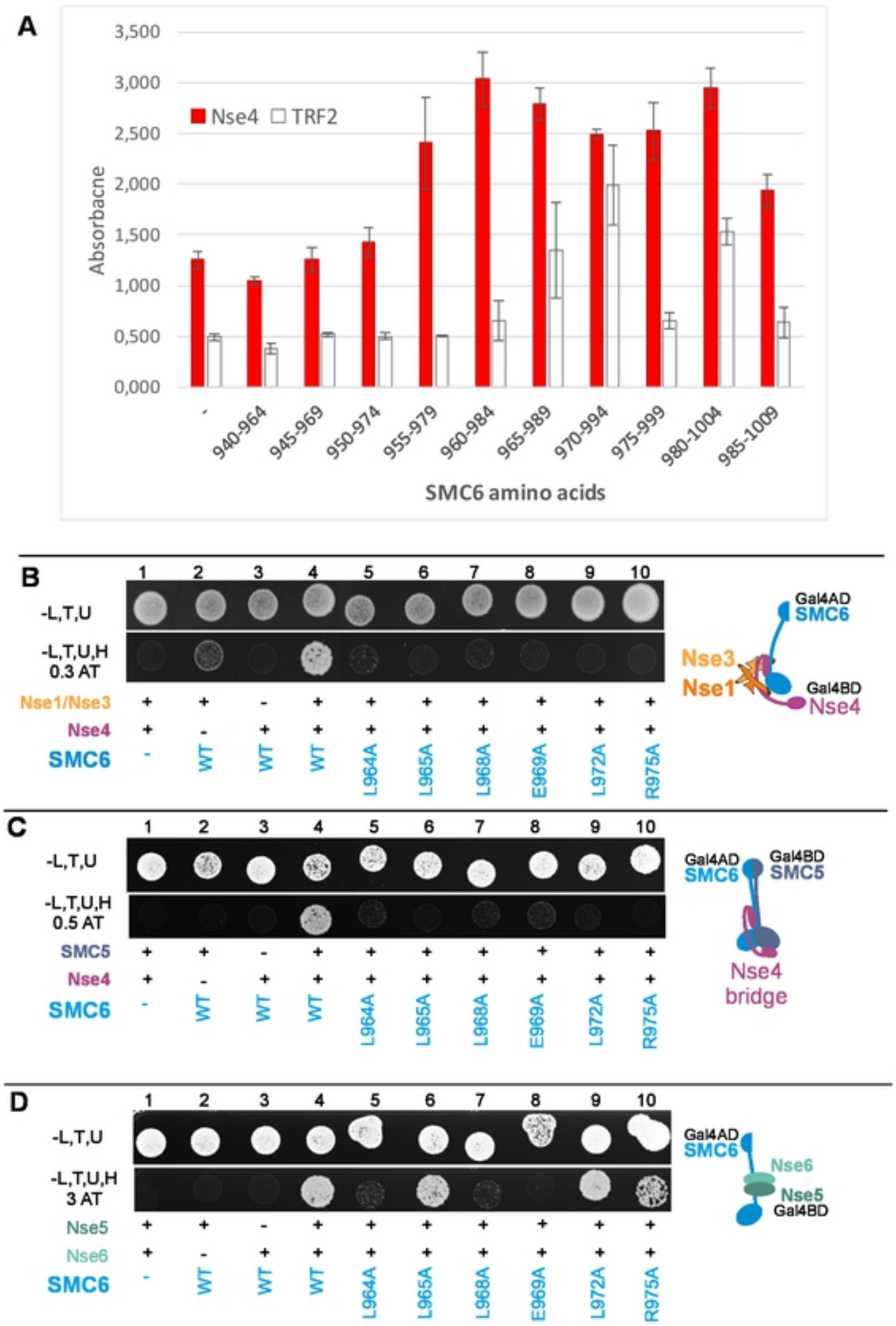
A
Nse4
TRF2
Absorbacne
3,500
3,000
2,500
2,000
1,500
1,000
0,500
0,000
-
940-964
945-969
950-974
955-979
960-984
965-989
970-994
975-999
980-1004
985-1009
SMC6 amino acids
B
1 2 3 4 5 6 7 8 9 10
-L,T,U
-L,T,U,H
0.3 AT
Nse1/Nse3 + + - + + + + + + +
Nse4 + - + + + + + + + +
SMC6 - WT WT WT L964A L965A L968A E969A L972A R975A
Gal4AD
SMC6
Nse3
Nse1
Gal4BD
Nse4
C
1 2 3 4 5 6 7 8 9 10
-L,T,U
-L,T,U,H
0.5 AT
SMC5 + + - + + + + + + +
Nse4 + - + + + + + + + +
SMC6 - WT WT WT L964A L965A L968A E969A L972A R975A
Gal4AD
SMC6
Gal4BD
SMC5
Nse4
bridge
D
1 2 3 4 5 6 7 8 9 10
-L,T,U
-L,T,U,H
3 AT
Nse5 + + - + + + + + + +
Nse6 + - + + + + + + + +
SMC6 - WT WT WT L964A L965A L968A E969A L972A R975A
Gal4AD
SMC6
Nse6
Nse5
Gal4BD

Figure 1

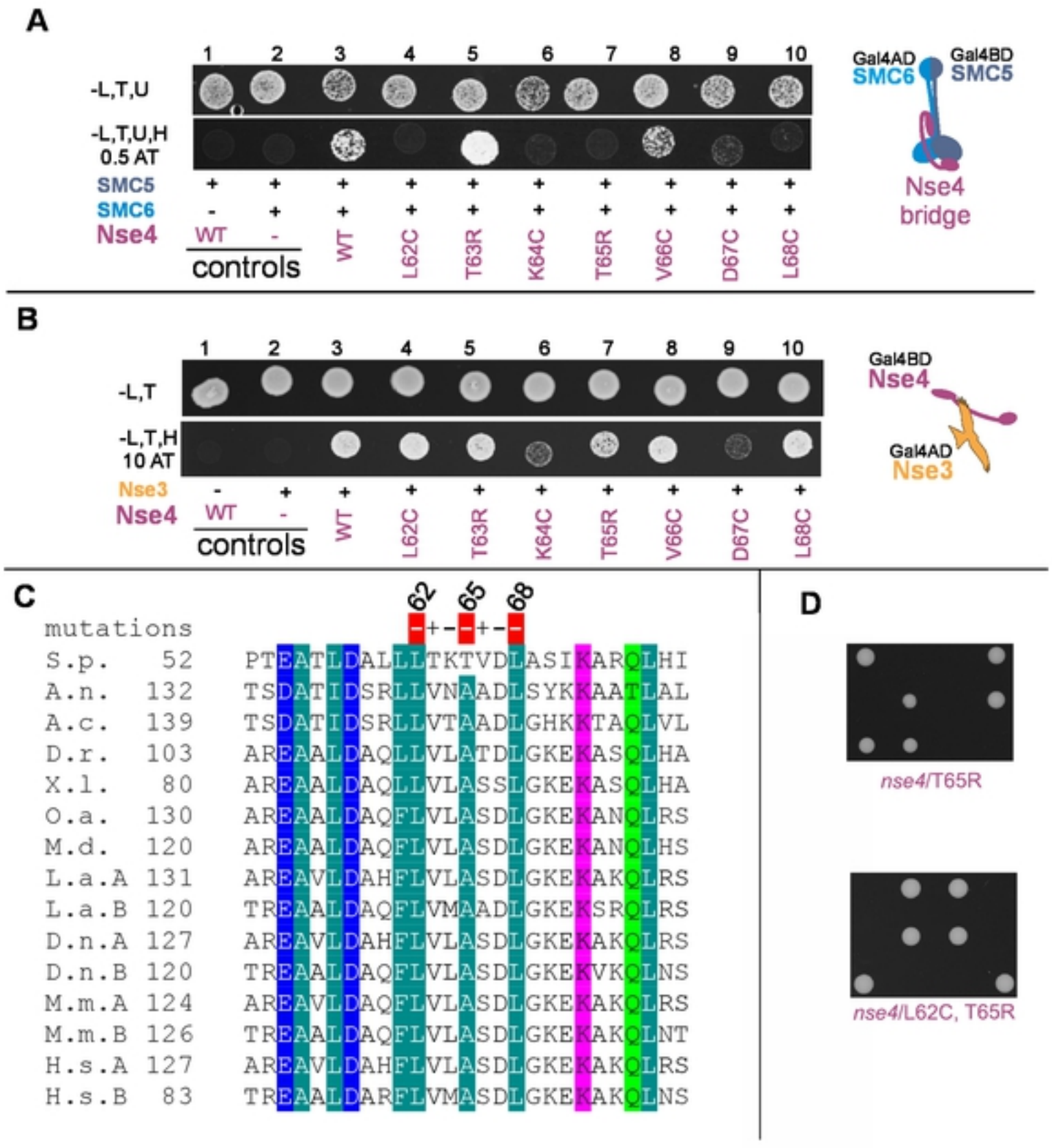
A
1 2 3 4 5 6 7 8 9 10
-L,T,U
-L,T,U,H
0.5 AT
SMC5
SMC6
Nse4
WT
controls
L62C
T63R
K64C
T65R
V66C
D67C
L68C
Gal4AD
SMC6
Gal4BD
SMC5
Nse4
bridge
B
-L,T
-L,T,H
10 AT
Nse3
Gal4BD
Nse4
Gal4AD
Nse3
C
mutations
62
65
68
S.p. 52 PTEATLDALLLTKTVDLASIKARQLHI
A.n. 132 TSDATIDSRLLVNAADLSYKKAATLAL
A.c. 139 TSDATIDSRLLVTAADLGHKKTAQLVL
D.r. 103 AREAALDAQLLVLATDLGKEKASQLHA
X.l. 80 AREAALDAQLLVLASSLGKEKASQLHA
O.a. 130 AREAALDAQFLVLASDLGKEKANQLRS
M.d. 120 AREAALDAQFLVLASDLGKEKANQLHS
L.a.A 131 AREAVLDAHFLVLASDLGKEKAKQLRS
L.a.B 120 TREAALDAQFLVMAADLGKEKSRQLRS
D.n.A 127 AREAVLDAHFLVLASDLGKEKAKQLRS
D.n.B 120 TREAALDAQFLVLASDLGKEKVKQLNS
M.m.A 124 AREAVLDAQFLVLASDLGKEKAKQLRS
M.m.B 126 TREAALDAQFLVLASDLGKEKAKQLNT
H.s.A 127 AREAVLDAHFLVLASDLGKEKAKQLRS
H.s.B 83 TREAALDARFLVMASDLGKEKAKQLNS
D
nse4/T65R
nse4/L62C, T65R

Figure 2

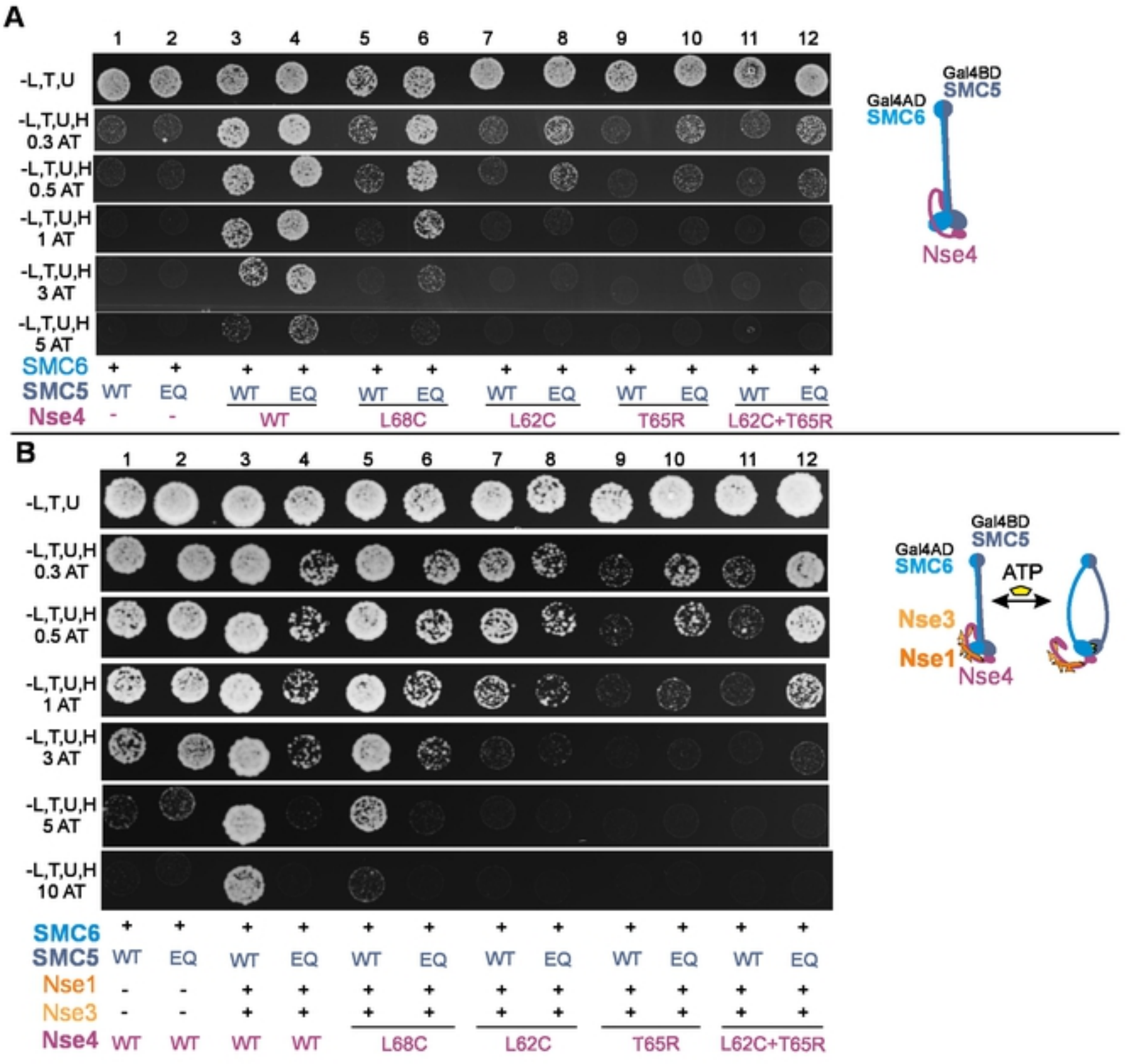
A
1 2 3 4 5 6 7 8 9 10 11 12
-L,T,U
-L,T,U,H 0.3 AT
-L,T,U,H 0.5 AT
-L,T,U,H 1 AT
-L,T,U,H 3 AT
-L,T,U,H 5 AT
SMC6 + + + + + + + + + + + +
SMC5 WT EQ WT EQ WT EQ WT EQ WT EQ WT EQ
Nse4 - - WT L68C L62C T65R L62C+T65R
Gal4BD SMC5
Gal4AD SMC6
Nse4
B
1 2 3 4 5 6 7 8 9 10 11 12
-L,T,U
-L,T,U,H 0.3 AT
-L,T,U,H 0.5 AT
-L,T,U,H 1 AT
-L,T,U,H 3 AT
-L,T,U,H 5 AT
-L,T,U,H 10 AT
SMC6 + + + + + + + + + + + +
SMC5 WT EQ WT EQ WT EQ WT EQ WT EQ WT EQ
Nse1 - - + + + + + + + + + +
Nse3 - - + + + + + + + + + +
Nse4 WT WT WT WT L68C L62C T65R L62C+T65R
Gal4BD SMC5
Gal4AD SMC6
ATP
Nse3
Nse1
Nse4

Figure 3

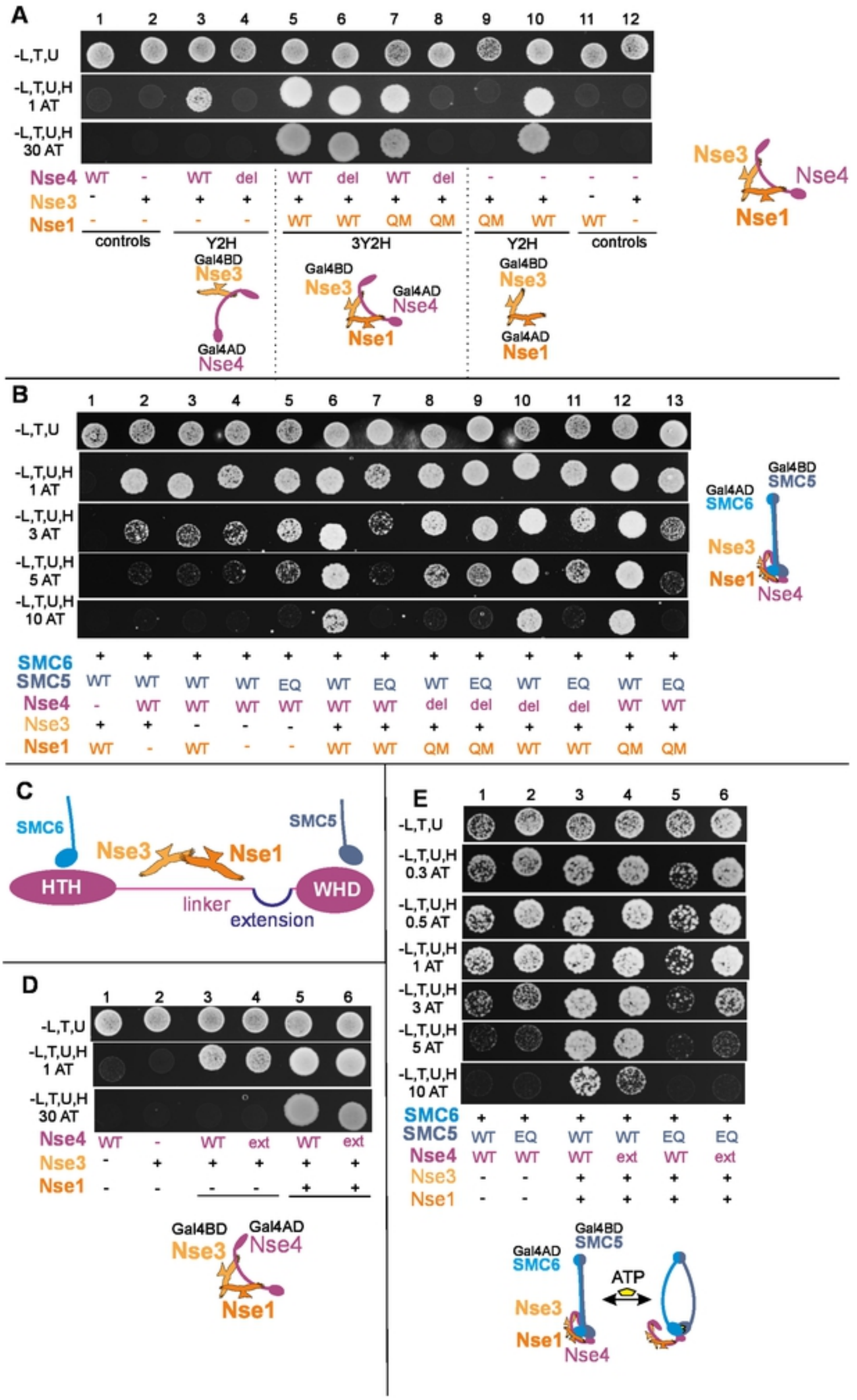
A
-L,T,U
-L,T,U,H 1 AT
-L,T,U,H 30 AT
Nse4
Nse3
Nse1
controls
Y2H
3Y2H
Y2H
controls
Gal4BD
Gal4AD
Nse3
Nse4
Nse1
B
-L,T,U
-L,T,U,H 1 AT
-L,T,U,H 3 AT
-L,T,U,H 5 AT
-L,T,U,H 10 AT
SMC6
SMC5
Nse4
Nse3
Nse1
Gal4BD
Gal4AD
C
SMC6
SMC5
Nse3
Nse1
HTH
WHD
linker
extension
D
-L,T,U
-L,T,U,H 1 AT
-L,T,U,H 30 AT
Nse4
Nse3
Nse1
Gal4BD
Gal4AD
E
-L,T,U
-L,T,U,H 0.3 AT
-L,T,U,H 0.5 AT
-L,T,U,H 1 AT
-L,T,U,H 3 AT
-L,T,U,H 5 AT
-L,T,U,H 10 AT
SMC6
SMC5
Nse4
Nse3
Nse1
Gal4BD
Gal4AD
ATP

Figure 4